Characterization of Protein Aggregates and Sub-visible Particles in Therapeutic Protein Formulations using ImageStream^X

Christine E. Probst[1], Brian E. Hall[1], David A. Basiji[1].
[1]Amnis Corp. (a part of EMD Millipore), 645 Elliott Ave W., Suite 100, Seattle, WA, 98119.

ABSTRACT

Protein aggregates (PA) and other types of sub-visible particles present within therapeutic protein formulations may impact drug safety and efficacy. USP <788> guidelines define limits for particles ≥ 10 µm, however characterization of particles 2-10 µm is increasingly expected based on their potential immunogenicity. Accepted industry techniques light obscuration and flow microscopy provide particle size and concentration information, but offer limited ability to differentiate among the different types of contaminants routinely found in therapeutic formulations. ImageStream^X (IS^X) imaging flow cytometry is a potentially attractive platform for analysis of sub-visible particles based on its ability to rapidly collect robust, single-particle data sets consisting of multispectral brightfield (BF), side-scatter (SSC), and fluorescent imagery. Herein we evaluate IS^X as a novel methodology for identification of three common particulate species- protein aggregates, silicone oil droplets (SO), and bacteria- using fluorescent labelling to identify particle type. Particle data was collected on IS^X and current industry standards HIAC liquid particle counter and Micro-Flow Imaging™ (MFI). The results demonstrate IS^X provides more sensitive detection of aggregates and facilitates identification of particles and their complexes using fluorescent tracers. IS^X should prove instrumental for developing processes that minimize drug degradation and understanding the role of particles on patient health.

Materials and Methods

Materials
ProteoStat® protein aggregation assay and ProteoStat® protein aggregation standards were kindly provided by Enzo Life Sciences (Farmingdale, New York). Silicone oil was purchased from Sigma Aldrich (Milwaukee, WI). BODIPY® 493/503 and SYTO® 62 Red Fluorescent Nucleic Acid Stain were purchased from Life Technologies (Carlsbad, CA), and were used to label SO and bacteria respectively.

Sample preparation
A SO emulsion (0.02% w/v) was prepared by mixing 5 µL silicone oil with 25 mL PBS and vortexing vigorously for one minute. ProteoStat protein aggregation standards are the only commercially available PA standards and were used as model experimental samples for this study. IgG aggregates were generated using heat and pH treatment, and individual standards were prepared by diluting aggregates in monomeric IgG in decreasing ratios and lyophilized. PA standards were reconstituted according to the manufacturers protocol to final PA concentrations of 125, 62.5, 31.3, 15.6, 7.8 3.9, 2.0, 1.0, 0.5, and 0 (0.1 µm filtered) µg/mL; 0.2 µm filtered H2O was used as a particle-free control. *Escherichia coli* (*E. coli*) were used as a model bacteria.

Fluorescence staining
A staining cocktail was prepared in 1x ProteoStat assay buffer at the following concentrations: 1.5 µM BODIPY, 1.25 µM SYTO 62, 1:4 dilution ProteoStat Detection reagent (note: manufacturer does not disclose the structure of this dye and thus the concentration is provided in units of 'x'). Experimental samples were fluorescently labelled by mixing with an equal volume of staining cocktail and incubated for 30 minutes prior to measurement on the IS^X.

Image acquisition
An IS^X MK II equipped with 12 image channels, or an IS^X equipped with 6 channels were used to perform particle analysis on samples (EMD Millipore, Seattle, WA). Both systems were equipped with 488 and 642 nm fluorescence excitation lasers, a 785 nm side scatter (SSC) laser, and modular 20/40/60x magnification objectives. Data for each sample was acquired for a minimum of 2,000 events or 5 minutes.

Data analysis using IDEAS
Image analysis was completed using Image-based algorithms using the IDEAS 6.0 image analysis software package.

Figure 1: Photo of ImageStream®^{X} MK II

Fluorescence labelling of PA, SO, and bacteria

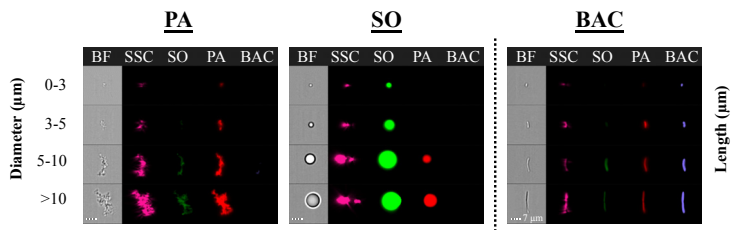

Figure 2: Multispectral imagery of PA, SO, and bacteria (BAC) collected on the IS^X following fluorescent labelling. Representative images for particles of increasing diameter are shown. Magnification: 60x. Scale bar, 7 µm.

Detecting interaction between PA and SO

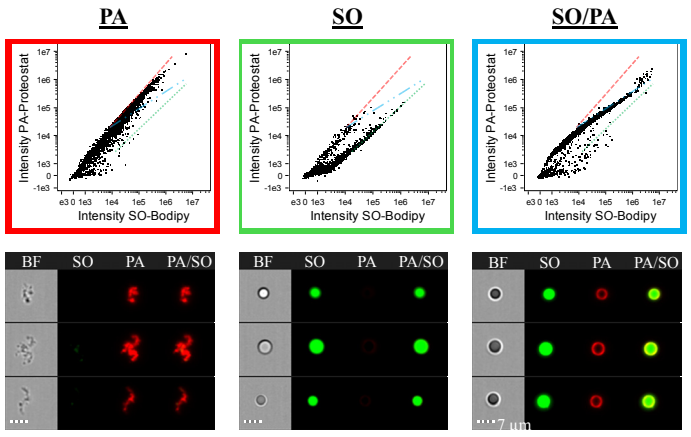

Figure 3: Protein adsorbs to surface of SO. Bivariate plots of SO-BODIPY vs. PA-ProteoStat Intensity shown for PA only, SO only, and SO mixed with monomeric protein. Reference lines are overlaid onto each plot to indicate the position of SO (green), PA (red), and SO with adsorbed protein (blue) for cross-sample comparison. Representative multispectral images are shown below each dot plot. Magnification: 60x. Scale bar, 7 µm.

PA vs. SO classification accuracy

$$Sensitivity = \frac{\#\,True\ Positives}{\#\,True\ Positives + \#\,False\ Negatives}$$

$$Specificity = \frac{\#\,True\ Negatives}{\#\,True\ Negatives + \#\,False\ Positives}$$

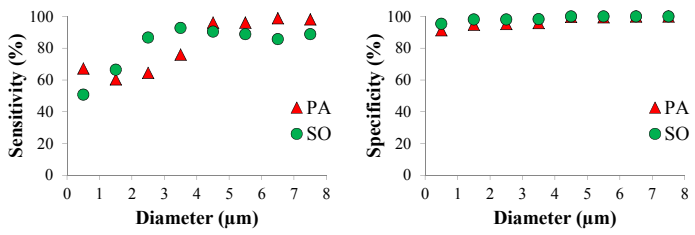

Figure 4: Effect of particle size on classification sensitivity and specificity for PA and SO. Values calculated for particle diameter ranging from 0-8 µm using 1 µm bins.

Identification of heterogeneous particle complexes

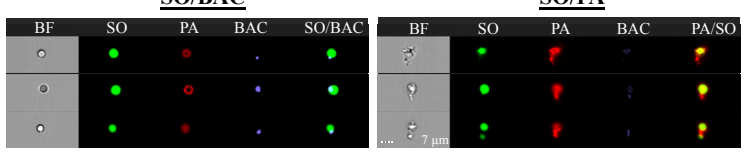

Figure 5: Representative multispectral images of heterogeneous particle-particle complexes, including SO with adherent bacteria, and PA with adherent SO. Magnification: 60x. Scale bar, 7 µm.

IS^X linear dynamic range for PA detection

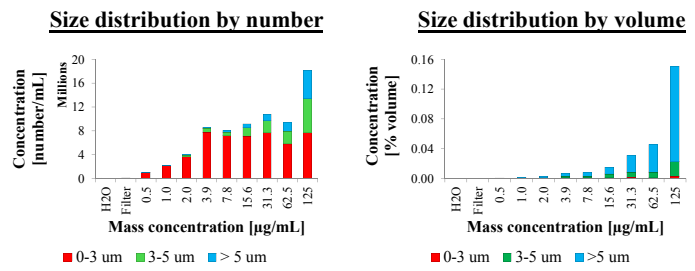

Figure 6: Dynamic range of particle concentrations detectable on the IS^X. Size distributions shown by number and volume for standards with increasing PA mass concentration. Concentration by volume is linearly proportional to mass concentration (R^2= 0.96).

Cross-platform sensitivity: IS^X, HIAC, MFI

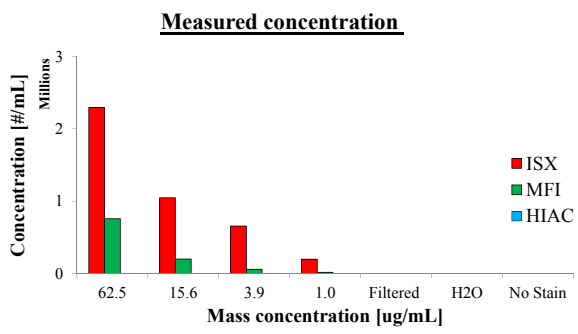

Figure 7: Cross-platform particle counts for samples with decreasing PA concentration

Sensitivity	Concentration (µg/mL)			
Fold increase (x)	62.5	15.6	3.9	1.0
MFI*	3.0	5.2	11.1	10.7
HIAC	510	924	624	516

Specificity	Control sample		
Counts (#/mL)	Filtered	H_2O	No Stain
ISX	3961	171	0
MFI	992	738	568
HIAC	43	28	47

Table 1: Instrument sensitivity and specificity for PA detection. Sensitivity determined by fold-increase in counts measured with IS^X compared to MFI and HIAC; specificity determined by counts measured in background samples. *Background subtracted.

Image quality for PA collected on IS^X vs. MFI

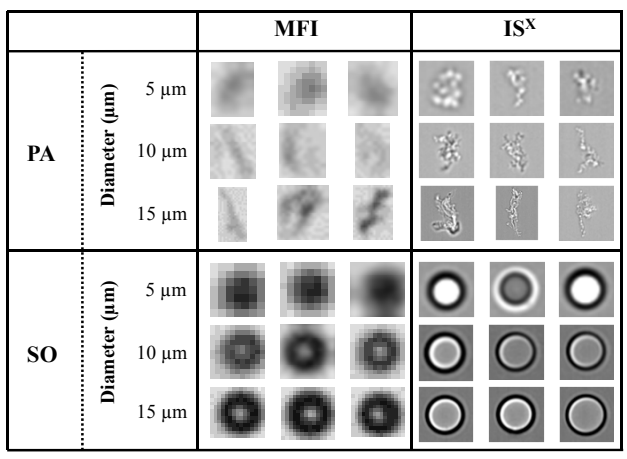

Figure 8: Representative brightfield images of SO and PA of increasing diameter collected on IS^X (60x) and MFI (14x) scaled to the same image size.

CONCLUSIONS

In this study, we demonstrate multiplexed detection and quantitation aggregates and other types of sub-visible particles routinely found in therapeutic protein formulations. A simple, wash-free, protocol was developed to label PA, SO, and bacteria using spectrally distinct fluorescent probes. IS^X analysis demonstrated that fluorescent probes were specific to each particle species (Fig. 2), however protein adsorption to the surface of SO caused overlap in the fluorescent properties of small particles (Fig. 3). Because PA and SO have distinct morphologies, particle classification was performed using a combination of morphological and fluorescent features selected through a classification algorithm available in IDEAS. Classifier accuracy was quantified as a function of particle size, resulting in specificity exceeding 90% for particles greater than 1 µm and sensitivity exceeding than 90% for particles greater than 4 µm (Fig. 4). Heterogeneous particle complexes were identified to illustrate the unique potential for the IS^X to investigate particle-particle interactions (Fig. 5). IS^X linear dynamic range was measured using aggregated IgG standards from 5 to 125 µg/mL, and a linear relationship (R^2 = 0.96) was identified using concentration by volume across the interrogated range (Fig. 6). The sensitivity and specificity of IS^X for aggregate detection was compared to current industry standards HIAC and MFI. Particle counts for samples containing PA were significantly higher using IS^X compared to MFI (~3-11x) and HIAC (~510-924x), while counts for the particle-free sample were significantly lower with IS^X compared to MFI (Fig. 7). Image quality was better for particles analyzed with IS^X compared to MFI due to higher magnification capabilities (60x vs. 14x) (Fig. 8) . The results from this pilot study indicate that IS^X overcomes many limitations of current methods used for particle analysis of therapeutics and provides opportunities for novel applications.